

Habitat loss and fragmentation increase realized predator-prey body size ratios

Jasmijn Hillaert¹, Martijn L. Vandegehuchte¹, Thomas Hovestadt², Dries Bonte¹

¹Department of Biology, Terrestrial Ecology Unit, Ghent University, K. L. Ledeganckstraat 35, 9000 Ghent,
Belgium

²Department of Animal Ecology and Tropical Biology, Biocenter, University of Wuerzburg, Fisher Str. 32, 97074
Wuerzburg, Germany

Corresponding author

Jasmijn Hillaert
Terrestrial Ecology Unit
Department of Biology
Ghent University
K. L. Ledeganckstraat 35
9000 Ghent
Belgium
Tel: +3292645258
e-mail: Jasmijn.Hillaert@ugent.be

1 *Abstract*

2

3 In the absence of predators, habitat fragmentation favors large body sizes in primary consumers with
4 informed movement due to their high gap-crossing ability. However, the body size of primary
5 consumers is not only shaped by such bottom-up effects, but also by top-down effects as predators
6 prefer prey of a certain size. Therefore, higher trophic levels should be taken into consideration when
7 studying the effect of habitat loss and fragmentation on size distributions of herbivores.

8 We built a model to study the effect of habitat loss and fragmentation within a simple food
9 web consisting of (i) a basal resource that is consumed by (ii) a herbivore that in turn is consumed by
10 (iii) a predator. Our results highlight that predation may result in local accumulation of the resource
11 via top-down control of the herbivore. As such, the temporal and spatial variation of the resource
12 distribution is increased, selecting for increased herbivore movement. This results in selection of
13 larger herbivores than in the scenario without predator. As predators cause herbivores to be
14 intrinsically much larger than the optimal sizes selected by habitat fragmentation in the absence of
15 predators, habitat fragmentation is no longer a driver of herbivore size. However, there is selection
16 for increased predator size with habitat fragmentation as herbivores become less abundant, favoring
17 gap-crossing ability of the predator. Since herbivore and predator body size respond differently to
18 habitat loss and fragmentation, realized predator-herbivore body size ratios increase along this
19 fragmentation gradient. Our model predicts the dominance of top-down forces in regulating body
20 size selection in food webs and helps to understand how habitat destruction and fragmentation
21 affect overall food web structure.

22

23

24

25 *Introduction*

26 Body size represents a super trait, regulating almost any trait of an individual by its effect on
27 metabolic rate (Peters, 1983; Brown *et al.*, 2004; Fritschie and Olden, 2016; Brose *et al.*, 2017). As
28 such, an individual's behavior, ecology and function are constrained by its body size (Bartholomew,
29 1982; Peters, 1983; Brown *et al.*, 2004). For example, small individuals have short generation times
30 and low energetic requirements whereas large individuals have higher average speed of movement
31 and resource consumption (Peters, 1983; Hirt *et al.*, 2017).

32 Herbivore species can show different allocation strategies: either few large or many small herbivore
33 individuals can exist given a certain amount of resources (DeLong and Vasseur, 2012; Yeakel, Kempes
34 and Redner, 2018). This observation that the cost of total metabolic biomass is independent of body
35 size is known as the 'Energetic Equivalence Rule' (Atkins *et al.*, 2015; DeLong and Vasseur, 2012;
36 Yeakel, Kempes and Redner, 2018; Damuth, 1981). However, the total metabolic biomass of a
37 herbivore species is constrained by resource availability or bottom-up dynamics. Importantly, with
38 increasing trophic level, more complex size-dependent processes imply extra energetic and
39 mechanical constraints. For a predator, prey that is too small are difficult to locate and render little
40 energy, whereas prey that is too large might be hard to control and capture (Brose *et al.*, 2006;
41 Portalier *et al.*, 2018). In foraging theory, this trade-off is represented by a hump-shaped function for
42 predation rate, with a maximum at intermediate predator-prey ratios (Brose *et al.*, 2008). As such,
43 predator-prey body size ratios are optimized in relation to habitat, prey and predator type,
44 depending on the specific costs and constraints of the system (Brose *et al.*, 2006). Generally, these
45 constraints and limits result in predators that are larger than their prey (Brose *et al.*, 2006; Portalier
46 *et al.*, 2018), corresponding to one of the earliest observations in biology (Elton, 1927). By
47 preferentially consuming prey of specific sizes, predators thus exert top-down forces within a food
48 web (Howeth *et al.*, 2013). The emerging predator-prey body size ratios are theoretically
49 demonstrated to maximize food web stability (Emmerson and Raffaelli, 2004; Brose, Williams and

50 Martinez, 2006). In a tri-trophic food web (Otto et al., 2007), for instance, deviations from optimal
51 predator-prey body sizes lead to predator extinction or unstable overshooting dynamics by resource
52 accumulation (as described by the paradox of enrichment) (McCann, 2012). When predators are
53 much smaller than their prey, energetic demand will increase during foraging (higher mass-specific
54 metabolic rate with decreasing size), resulting in predator extinction by resource limitation (Otto et
55 al., 2008). On the contrary, when predators are much larger than their prey, prey will eventually be
56 suppressed, thereby giving rise to basal resource accumulation (Otto et al., 2008).

57 Because individual movement capacities and efficiencies are strongly related to energy use and body
58 size, the spatial distribution of resources will impose selection on body size (Allen *et al.*, 2006; Hirt et
59 al. 2018). Selection favors those individuals that move at a spatial scale at which resources are
60 abundant and ensure optimal resource access (Holling, 1992; Nash *et al.*, 2014; Raffaelli *et al.*, 2016).

61 Because of the current threat of habitat loss and fragmentation, many species are expected to
62 experience changes in the spatial organization of their habitat, and these are thought to be at the
63 basis of many observed body size shifts. Body size shifts due to habitat fragmentation are widely
64 documented in nature but so far not well understood (Lomolino and Perault, 2007; Braschler and
65 Baur, 2016; Renauld *et al.*, 2016; Warzecha *et al.*, 2016; Merckx *et al.*, 2018). Habitat loss refers to a
66 decrease in the amount of suitable habitat whereas fragmentation per se implies a decrease in the
67 spatial autocorrelation of suitable habitat (Jackson and Fahrig, 2013; Fahrig, 2017). It is important to
68 study both effects independently, as each has a distinct effect on species performance within multi-
69 trophic food webs (Liao, Bearup and Blasius, 2017). Habitat loss generally has negative effects on
70 species survival, whereas fragmentation might promote species coexistence within a trophic level by
71 lowering competition and between trophic levels by providing refuges (Jackson and Fahrig, 2013,
72 2015; Fahrig, 2017; Liao, Bearup and Blasius, 2017; Fletcher Jr *et al.*, 2018). So far, theoretical studies
73 have demonstrated that large individuals can be selected with increasing levels of isolation and
74 habitat fragmentation due to their high gap-crossing ability (Etienne and Olf, 2004; Hillaert,
75 Hovestadt, *et al.*, 2018). Within a resource-consumer context, however, this selection of large

76 individuals has only been observed in case of completely informed movement that lowers the risk of
77 arriving in unsuitable habitat (Hillaert, Vandegehuchte, *et al.*, 2018). Whether predators respond
78 similarly to habitat loss and fragmentation as their prey is unclear. While the resource of the prey is
79 stationary, the resource of the predator is mobile; selection on herbivore and predator size during
80 habitat loss and fragmentation may thus be different. Moreover, predators exert strong selection on
81 consumer body size by consuming only particular sizes according to their preferred optimal predator-
82 prey body size ratio (Howeth *et al.*, 2013; Tsai, Hsieh and Nakazawa, 2016). In order to consider the
83 top-down effect of the predator on consumer selection, it is essential to include food web topology
84 in studies of species responses to habitat fragmentation (Liao, Bearup and Blasius, 2017).
85 Importantly, differential body size responses across trophic levels might shift realized predator-prey
86 body size ratios (Tsai, Hsieh and Nakazawa, 2016), thus affecting predator-prey interaction strength
87 (Emmerson and Raffaelli, 2004).

88 As mentioned before, theory so far focused on how body mass distribution shifts within one trophic
89 level (Milne *et al.*, 1992; Etienne and Olff, 2004; Buchmann *et al.*, 2011, 2013; Hillaert, Hovestadt, *et*
90 *al.*, 2018). However, this study does not include the effect of predation. To increase realism, we here
91 studied the effect of habitat loss and fragmentation on body size selection within a simple resource-
92 herbivore-predator model. This was achieved by extending the model presented in (Hillaert,
93 Vandegehuchte, *et al.*, 2018) with an extra trophic level. In this model, individual traits of the
94 herbivore and predator are described by established allometric rules (Peters, 1983). We focus on the
95 effect of habitat fragmentation at the scale of foraging while distinguishing the process of habitat
96 loss from the process of fragmentation per se. The scale of foraging is applied because fine-grained
97 fragmentation has a larger effect on individual survival and reproduction than coarse-grained
98 fragmentation when a species invests more time in foraging than dispersing (Cattarino, Mcalpine and
99 Rhodes, 2016). Our goal is to answer the following questions: (i) How does predation affect body size
100 selection in the herbivore? (ii) Do trophic levels respond differently to fine-scale habitat

101 fragmentation and destruction? (iii) Which effects dominate: top-down or bottom-up? (iv) Are

102 realized predator-prey body size ratios affected by fine-scale habitat fragmentation and destruction?

103

104 *Material and methods*

105 We here took an arthropod-centered approach and parameterized allometric rules for a herbivore
106 and predator that are both haploid and parthenogenetic with a semelparous lifecycle.

107 By applying an individual-based approach, we were able to include intra-specific size variation and
108 stochasticity within our model. This approach in conjunction with the assumption of asexual
109 reproduction and equivalent ontogenetic and interspecific scaling exponents (West, Brown and
110 Enquist, 2001; Moses *et al.*, 2008), implies that our results can be interpreted both at the
111 metapopulation and metacommunity level for both the herbivore and the predator. A detailed
112 description of the model following the ODD (Overview, Design concepts and Details) protocol is
113 available in supplementary material part 1 (Grimm *et al.*, 2010). The applied model is based on
114 Hillaert, Vandegehuchte, *et al.* (2018).

115 *The landscape*

116 The landscape is a cellular grid of 200 by 200 cells and is generated using the Python package NLMpy
117 (Etherington, Holland and O'Sullivan, 2015). Each cell within the landscape has a side length (SL) of
118 0.25 m and therefore a total surface of 0.0625 m². Within the landscape, a distinction is made
119 between suitable and unsuitable habitat. Only within suitable habitat, the basal resource is able to
120 grow. When testing the effect of landscape configuration, the proportion of suitable habitat (P) and
121 habitat autocorrelation (H) were varied between landscapes. Habitat availability increases with P ,
122 whereas habitat fragmentation decreases with H . The following values were assigned to P : 0.05, 0.20,
123 0.50 or 0.90. H equaled either 1 (in all four cases), 0.5 (when P equaled 0.05 or 0.20) or 0 (when P
124 equaled 0.05). As such, highly fragmented landscapes with a high amount of suitable habitat were
125 not included in the analysis as these rarely occur in nature (Neel, McGarigal and Cushman, 2004).

126 *The basal resource*

127 Local resource biomass is represented as the total energetic content of resource tissue within that
128 cell ($R_{x,y}$ in Joule). This resource availability grows logistically in time depending on the resource's

129 carrying capacity (K) and intrinsic growth rate (r). In any cell, a fixed amount of resource tissue (E_{nc} , in
130 Joules, fixed at $2 J$) is non-consumable by the herbivore species, representing below-ground plant
131 parts. As such, E_{nc} is the minimum amount of resource tissue present within a suitable cell, even
132 following local depletion by the herbivore species.

133 Herbivore and predator

134 All herbivores and predators are modelled as individuals within the landscape. Both, herbivore and
135 predator develop through two life stages: a juvenile and adult life stage. Within a day, both stages
136 have the chance to execute different events (see Figure 1). Each day an individual executes all these
137 events sequentially. The order in which individuals (herbivores and predators) are selected is
138 randomized daily. Importantly, during the consumption event, the herbivore feeds on the basal
139 resource whereas the predator feeds on the herbivore.

140 First, an individual nourishes its energy reserve by resource consumption and predating. Second, the
141 energy reserve is depleted by the cost of daily maintenance (i.e. basal metabolic rate) and the cost of
142 movement. Third, juveniles further deplete the energy reserve by growth, eventually resulting in
143 maturation if they reach their adult size (W_{max}). Energy that was not utilized is stored within the
144 energy reserve. Adults can only reproduce if their internally stored energy (E_r) exceeds a predefined
145 amount. As the herbivore species and the predator species are semelparous, adults die after
146 reproduction.

147 In both the herbivore and the predator, an individual's body size at maturity (W_{max} , in kg) is coded by
148 a single gene. Adult size is heritable and may mutate with a probability of 0.001 during reproduction.
149 A new mutation is drawn from the uniform distribution $[W_{max} - (W_{max}/2), W_{max} + (W_{max}/2)]$ with W_{max}
150 referring to the adult size of the parent. New mutations may not exceed the predefined boundaries
151 $[0.01g, 3g]$ that represent absolute physiological limits. Both minimum and maximum weight are
152 similar for the predator and the herbivore. New variants of this trait may also originate by

153 immigration (see immigration below). Mutation enables fine-tuning of the optimal body size,
154 whereas immigration facilitates fitness peak shifts.

155 Initialization

156 For any parameter combination, 50 simulations were run. At the start of a simulation, adult
157 individuals were introduced with an average density of one herbivore per two suitable cells. After 20
158 timesteps, 1000 predators are randomly added to the landscape in any suitable cell. This time lag
159 allows the herbivore to reach a stable population size, increasing predator survival chances. The
160 adult mass of each individual (W_{max}) (for both herbivores and predators) was defined as ten raised to
161 the power of a value drawn from the uniform interval [-5, -2.522878745]. In other words, we sample
162 a value between 0.00001 kg (minimum adult mass) and 0.003 kg (maximum adult mass). As such,
163 individuals with masses of different orders of magnitude have an equal chance of being initialized in
164 the landscape. Moreover, initialized distributions are skewed to small individuals. Initial resource
165 availability per cell was 100 J. Total runtime was 3000 time steps for all scenarios, with one time step
166 corresponding to one day.

167 Immigration

168 The frequency with which predator and herbivore immigrants arrive in the landscape is described by
169 q . This variable is fixed at one per 10 days. The process of determining an immigrant's adult mass is
170 similar as during initialization (see above). An immigrant is always introduced within a suitable cell
171 and its energy reserve contains just enough energy to cover the cost of basal metabolic rate and
172 movement during the first day.

173 The implementation of body size

174 The assumptions describing the daily events of the herbivore are described in the resource-consumer
175 model (Hillaert, Vandegehuchte, *et al.*, 2018). Some events do not differ significantly between
176 trophic levels and are therefore assumed to be identical for the herbivore and the predator (this is
177 the case for basal metabolic rate, growth, maturation and reproduction. Details are provided in

178 (Hillaert, Vandegehuchte, *et al.*, 2018) and the ODD protocol in supplementary material part 1. The
179 events that differ between the predator and the herbivore are described below.

180 *Consumption*

181 Individual ingestion rate (IR , in Watts) of an individual increases with its size (W , in kg) by the
182 following equation for both the herbivore and the predator:

$$183 \quad IR = 2 * W^{0.80} \text{ (eq. 1)}$$

184 Following log transformation, the slope (0.80) was found by Peters (1983) to be the mean of several
185 studies focusing on ingestion rates of poikilotherms (Peters, 1983). The intercept of this equation lays
186 within the observed range of elevations [0.12 to 2] of these studies (Peters, 1983).

187 Based on eq. 1, the amount of energy ingested per day for an individual (i_{max} in Joules) is determined
188 as

$$189 \quad i_{max} = 2 \cdot W^{0.80} \cdot t_f \text{ (eq. 2)}$$

190 with t_f referring to the time devoted per day to consumption (in seconds), which is fixed at 15 hours.

191 The herbivore

192 The amount of resources consumed by a herbivore (E_c) only equals i_{max} if this amount is available.
193 Otherwise, E_c equals the amount present within a cell. As such, we assume contest competition for
194 resources, with a competitive advantage for those individuals which are randomly selected first
195 during a day.

196 When we consider that the herbivore feeds on young terrestrial foliage, it can only assimilate 65
197 percent of its daily ingested energy (Ricklefs, 1974 cited in Peters, 1983). Moreover, we assume that
198 the herbivore loses 10 percent of its ingested energy to processing costs (i.e. specific dynamic action)
199 (Ricklefs, 1974). As such, only 55 percent of the ingested energy remains available to the organism.
200 Therefore, the energy that is being assimilated by a herbivore individual (E_o in Joules) is described by

201
$$E_a = 0.55 \cdot E_c \text{ (eq. 3)}$$

202

203 The predator

204 For each predator, the herbivore individuals located within its cell are selected within a random
205 order. Per selected herbivore, the chance of successful attack (s_a) is calculated. This chance is defined
206 by multiplying the chance of interaction based on herbivore abundance (i_{PH}) with a measure for
207 optimality of the predator-herbivore body size ratio (O_{BSR}):

208
$$s_a = i_{PH} \cdot O_{BSR} \text{ (eq. 4).}$$

209 i_{PH} increases with herbivore abundance in a cell, according to:

210
$$i_{PH} = \frac{1}{1 + e^{-\frac{1}{4}(N_H - 11)}} \text{ when } N_H > 0 \text{ (eq. 5)}$$

211 with N_H representing the number of herbivores present within a cell, being continuously updated
212 during a day. This function has a sigmoid shape and therefore implies a functional type III response
213 (see Figure 2), stabilizing food web dynamics as highlighted by the sensitivity analysis (see
214 supplementary material part 2). During a day, the number of herbivores present in a cell (N_H) is
215 constantly updated.

216 Contrary to a preferred predator- prey body mass ratio which depends on predator body mass, we
217 included a fixed ratio which is in line with (Tsai, Hsieh and Nakazawa, 2016). Per selected predator-
218 herbivore pair, the corresponding \log_{10} (predator-herbivore body mass ratio) is calculated. This ratio
219 is then compared with the observed distribution of \log_{10} (predator-prey body mass ratios) in
220 terrestrial systems with invertebrate predators (normal distribution with average 0.6 and SD 1.066)
221 (Brose *et al.*, 2006). We refer to this observed distribution as the preferred predator-herbivore body
222 mass ratio (Tsai *et al.*, 2016). If the ratio of the selected pair is rarely observed in nature, the value for
223 O_{BSR} is close to zero. In case the ratio is often observed, the value for O_{BSR} lays close to 1. In order to

224 obtain values for O_{BSR} between 0 and 1, the observed normal distribution in nature is scaled by an
225 extra factor. As such, the formula for the calculation of O_{BSR} is the following (see Figure 3):

$$226 \quad O_{BSR} = \frac{\frac{1}{1.066 \cdot \sqrt{2\pi}} e^{-\frac{1}{2} \left(\frac{\log_{10} \left(\frac{W_{predator}}{W_{herbivore}} \right) - 0.6}{1.066} \right)^2}}{\frac{1}{1.066 \cdot \sqrt{2\pi}}} \quad (\text{eq. 6}).$$

227 As i_{PH} and O_{BSR} are both numbers within the interval [0,1], the same is true for s_a . In case a randomly
228 sampled number from the interval [0,1] is smaller than s_a , the attack of the predator on the
229 herbivore is successful and E_c of the predator is increased with $W_{t,herbivore} * 7000000 + E_{r,herbivore}$. This
230 formula assumes that the energetic content of wet tissue corresponds to 7×10^6 Joule per kg (Peters,
231 1983) and that the body mass of a herbivore ($W_{t,herbivore}$) does not include the energy stored within its
232 energy reserve (E_r). As long as E_c is smaller than i_{max} of the predator, another herbivore within the
233 same cell may be attacked by the predator. However, E_c does never exceed i_{max} .

234 Considering that the predator feeds on insects, it may assimilate 80 percent of its daily ingested
235 energy (Ricklefs, 1974; Peters, 1983). However, we assume that the predator loses 25 percent of its
236 ingested energy to processing costs (i.e. specific dynamic action) (Ricklefs 1974 cited in Peters 1983).
237 As such, only 55 percent of the ingested energy remains available to the organism. Therefore, the
238 energy that is being assimilated by a predator individual (E_a in Joules) is described by the same
239 formula as for the herbivore (see eq. 3).

240 *The movement phase*

241 *Probability of moving (p)*

242 Whether an individual moves, depends on the ratio of the amount of energy present within a cell
243 relative to the amount of energy it can eat during a day (i_{max}).

244 The probability of moving (p) for a herbivore is thereby calculated as, based on Poethke and
245 Hovestadt, 2002 :

$$246 \quad p_{herbivore} = 1 - \frac{R_{x,y}}{i_{max}} \quad \text{if } \frac{R_{x,y}}{i_{max}} < 1 \quad (\text{eq. 7})$$

247
$$p_{herbivore} = 0 \quad \text{if } \frac{R_{x,y}}{i_{max}} \geq 1.$$

248 A predator's probability of moving is based on s_a : the chance of moving decreases with the chance of
249 successful attack by

250
$$p_{predator} = 1 - s_a \text{ (eq. 8).}$$

251 In the formula of s_a , the average herbivore mass within the cell is applied (see eq. 4 and 6).

252 Defining searching area

253 As one time step in our model corresponds to one day, we do not model the movement behavior of
254 an individual explicitly, but instead estimate the total area an individual can search for resources
255 during a day. This area is called an individual's searching area is calculated once per time step, for
256 each moving individual. As all cells within a particular distance from the origin are equally intensively
257 searched, the searching area is circular with a radius (rad) and a center corresponding to the current
258 location of an individual (Delgado *et al.*, 2014). An individual's searching area increases with an
259 individual's optimal speed (v_{opt}), movement time (t_m) and perceptual range (d_{per}). Both optimal speed
260 and perceptual range depend on body mass, resulting in larger searching areas for larger individuals.
261 The cost of movement includes the energy invested by an individual in prospecting its total searching
262 area. Therefore, it is dependent on the size of the total searching area instead of the shortest
263 distance between the cell of origin and cell of destination.

264 An individual's optimal speed of movement (v_{opt} , in meters per second) is calculated for herbivores
265 according to the following equation, derived for walking insects (Buddenbrock, 1934; Peters, 1983):

266
$$v_{opt, herbivore} = 0.3 \cdot W^{0.29} \text{ (eq. 9)}$$

267 Speed of movement (v_{opt} , in meters per second) of the predator is defined by the following equation
268 (Hirt *et al.*, 2017):

269
$$v_{opt, predator} = 1.0045 \cdot W^{0.42} \text{ (eq. 10).}$$

270 The time an individual invests in movement per day (t_m , in seconds) is maximally 1 hour. In case too
271 little internally stored energy is present to support movement for one hour, t_m is calculated by:

272
$$t_m = \frac{E_r}{c_m} \text{ (eq. 11).}$$

273 c_m refers to the energetic cost of movement (in joules per second) and is calculated for herbivores by
274 the following formula, which is based on running poikilotherms (Buddenbrock, 1934; Peters, 1983)):

275
$$c_{m, \text{ herbivore}} = (0.17W^{0.75} + 3.4W) \text{ (eq. 12).}$$

276 We adapt the formula of c_m for the predator by implementing the formula for $v_{opt, \text{ predator}}$ in the
277 formula of c_m (see supplementary material part 3 for derivation):

278
$$c_{m, \text{ predator}} = (0.17W^{0.75} + 11.35W^{1.14}) \text{ (eq. 13).}$$

279 The cost of moving during the time t_m ($c_m \cdot t_m$) is subtracted from an individual's energy reserve. Based
280 on t_m and v_{opt} , the total distance an individual covers at day t (d_{max}) is determined as:

281
$$d_{max} = v_{opt} \cdot t_m \text{ (eq. 14).}$$

282 Next, the perceptual range of an individual is determined by means of the following relationship:

283
$$d_{per} = 301W + 0.097 \text{ (eq. 15).}$$

284 For simplicity, this relationship is linear and based on the assumption that the smallest individual
285 (0.01g) has a perceptual range of 0.10 m and the largest individual (3g) a perceptual range of 1m. The
286 effect of this relationship has been tested (see supplementary material part 2). Moreover, the
287 positive relationship between body size and perceptual range or reaction distance has been
288 illustrated over a wide range of taxa, including arthropods (supplementary information of Pawar, Dell
289 and Van M. Savage, 2012).

290 The foraging area of an individual is circular and its radius (*rad*, in m) is calculated by taking into
291 account the total distance the individual has covered during the day and the individual's perceptual
292 range (see Supplementary material part 5 for explanation of this formula):

$$293 \quad rad = \sqrt{\frac{2 \cdot d_{max} \cdot d_{per} + \pi \cdot d_{per}^2}{\pi}} \text{ (eq. 16).}$$

294 In order to avoid side-effects of applying the variable *rad* for a continuous landscape within a cellular
295 landscape, a randomly drawn value from the following distribution, $[-0.5 \cdot SL, 0.5 \cdot SL]$, is added to
296 *rad*.

297 Habitat choice

298 Here, movement is informed as an individual always moves to the cell with the highest amount of
299 resources (the herbivore) or the cell with the highest rate of successful attack (based on average
300 herbivore weight per cell in case of the predator) within its foraging area.

301

302 Output

303 Only simulations in which the predator persists during the final 500 days of a simulation are included
304 in the analysis. An overview of the number of included simulations per landscape type is given in
305 Table S2.1. During each simulation, we traced changes in the mean amount of resources per cell and
306 total number of adults and juveniles and average adult mass (W_{max}) of both the herbivore and the
307 predator over time. Throughout the final 1500 days of a simulation, 1000 eggs (for predators and
308 herbivore each) were randomly selected to be followed during their lifetime. The movements and
309 reproductive success of the resulting herbivore individuals were recorded. During the final 100 days
310 of a simulation, the \log_{10} (predator-herbivore body mass ratio) was recorded per successful predation
311 event. As such, the average \log_{10} (predator-herbivore body mass ratio) could be determined per
312 scenario, as well as the deviation of this average from the implemented optimum \log_{10} (body mass
313 ratio).

314 At the end of a simulation, the body masses of maximally 50 000 predators and maximally 50 000
315 herbivores were randomly sampled. Also, the abundance of predators and herbivores as well as the
316 resource amount per cell was written out. This enables us to study the spatial distribution of the
317 predator(s), the herbivore(s) and the resource.

318 In order to determine the effect of the predator(s) on herbivore body weight distributions, the
319 settings of the resource-herbivore-predator model were applied to run a comparable model without
320 predator (see Table S1.1).

321

322 *Results*

323 In each landscape type, the body mass of the predator is selected to be higher than that of the
324 herbivore. Habitat loss, in conjunction with fragmentation, selects for an increase in average body
325 mass of the predator (Figure 4). Habitat loss within highly autocorrelated landscapes (H equaling 1),
326 does not clearly affect average predator body mass. However, the number of simulations in which
327 the predator and herbivore survive during the final 500 days of a simulation are lowest when P
328 equals 0.05 and H 1 or H 0.05 (Table S2.1). Although a similar pattern is observed for herbivore body
329 mass when no predator is present, herbivore body mass shows almost no response to habitat
330 fragmentation in the presence of a predator. This pattern is always supported by the sensitivity
331 analysis, except for the scenario with a clutch size of 2. Furthermore, in case of P 0.05 and H 1,
332 average predator body mass sometimes approaches that of the scenario with P 0.05 and H 0. When
333 this is the case, the number of included simulations is low due to extinction of the predator.
334 Moreover, in this landscape type (P 0.05 and H 1), drift is strong, explaining the variation in average
335 body mass between simulations. Notably, the body mass of a herbivore is overall larger when a
336 predator population or community is present, except for the landscape with P equaling 0.05 and H 0.

337 Temporal and spatial dynamics of the resource and the herbivore are strongly affected by the
338 presence of a predator, illustrating the strength of the top-down force. Dynamics within the
339 predator-herbivore-resource food web fluctuate strongly over time (Fig S4.1). Moreover, the spatial
340 distribution of the resource and the herbivore is highly heterogeneous (Fig 5). When a predator is
341 present, the number of suitable patches occupied by the herbivore is lower (Fig S4.2). Also, the
342 average amount of resources per cell is higher (Fig S4.3), and even local accumulation occurs (Fig 5).
343 Importantly, top-down and bottom-up forces strongly interact in our model. For example, resources
344 increase in abundance with habitat fragmentation and destruction when a predator is not present
345 (Fig S4.3). In contrast, habitat fragmentation and destruction result in a decrease in resource amount
346 when a predator is present (Fig S4.3).

347 The average realized \log_{10} (predator-herbivore body mass ratio) strongly approximates the preferred
348 ratio when P equals 0.9 and H equals 1 (Figure 6). However, with increasing habitat loss and
349 fragmentation, the realized \log_{10} (predator-herbivore body mass ratio) is selected to increase, up to a
350 maximum at $P = 0.05$ and $H = 0$ (Figure 6). This deviation from the preferred ratio with increasing
351 habitat loss and fragmentation is strongly confirmed by the sensitivity analysis (Table S4.1).
352 Moreover, the sensitivity analysis highlights that parameter changes that limit movement increase
353 the overall deviation (Table S4.1), while parameter changes that facilitate movement decrease the
354 deviation (e.g. higher value for t_m) (Table S4.1).

355

356

357 *Discussion*

358 First principles from movement ecology and metabolic theory predict how fine-grained habitat
359 fragmentation changes selection on body size within a simple three-trophic food web model. The
360 findings of our model are the following. (i) Predators induce a spatially and temporally
361 heterogeneous distribution of the resource, thereby selecting for increased movement (ability) and
362 thus increased size in herbivores. (ii) Predators cause herbivores to be intrinsically much larger than
363 the optimal sizes selected by habitat fragmentation in the absence of predators, so that habitat
364 fragmentation is no longer a driver of herbivore size. Since habitat fragmentation causes herbivore
365 abundance to decrease, it selects for a large predator size as larger predators are more mobile. (iii)
366 Body size distributions of primary consumers are largely regulated by top-down forces. (iv) The
367 realized predator-prey body size ratio increases with habitat fragmentation due to different selection
368 at different trophic levels.

369

370 *Effect of predators on herbivore size*

371 In the absence of predators, selection on herbivore body size has been demonstrated to depend on
372 the spatial organization of resources, and information use during movement (Hillaert,
373 Vandegehuchte, *et al.*, 2018). Without predator interactions, the optimal body mass of herbivores
374 that move in an informed way increases with habitat fragmentation and loss. Moreover, when the
375 percentage of suitable habitat is high, a herbivore's body mass is minimized. Under these conditions,
376 small herbivores are selected as these have the shortest generation times whereas no benefit results
377 from being able to cover a large spatial extent and, hence, from being large, as resources are
378 uniformly distributed in space. We here show that if a herbivore coexists with its predator, the
379 herbivore's temporal and spatial dynamics are much more unstable and resources become highly
380 heterogeneously distributed in space. This arises because predators can deplete local herbivore
381 populations, thereby enabling resource accumulation and generating high spatial and temporal

382 variability in resource levels. As such, selection acts in favor of those herbivores that can reach cells
383 with high amounts of resources first (Hastings, 1983). Hence, herbivores which move in an informed
384 way are selected to be larger in the presence than in the absence of a predator. Since Amarasekare
385 (2016) retrieved similar adaptive dynamics for dispersal in a simple tri-trophic foodweb, we can
386 conclude that, here, selection for enhanced movement is the main driver behind body size evolution.

387

388 [Effect of habitat fragmentation on body size across trophic levels](#)

389 In the absence of predators, herbivore size is selected to increase with habitat loss and
390 fragmentation (Hillaert, Vandegehuchte, *et al.*, 2018). This effect disappears in our tri-trophic model,
391 in the presence of predator-prey dynamics. Absence of a selection differential implies the presence
392 of a single optimal herbivore size irrespective of the resource's spatial organisation. As such,
393 herbivores shift towards larger sizes in the presence than in the absence of predators when
394 resources are abundant, but to smaller sizes when resources are rare and highly fragmented ($P > 0.05$
395 and $H > 0$). This inverse pattern can be explained by fitness disadvantages for the herbivore of being
396 too large, associated with an increased time until maturity and hence increased lifetime predation
397 pressure.

398 In contrast to the herbivore, the predator is always selected to be larger than the herbivore and,
399 more importantly, its average body size increases with habitat fragmentation. The model observation
400 that predators are larger than their prey follows logically from the implemented optimal predator-
401 herbivore body mass ratio as observed in nature. Too high or too low predator-prey body mass ratios
402 are not favorable as too small prey are hard to trace and offer low energy profit, whereas too large
403 prey may be hard to control and capture (Brose *et al.*, 2006; Brose, 2010; Portalier *et al.*, 2018).
404 Moreover, as predators need to keep track of mobile herbivores, selection on movement should
405 always be strong in active hunters. This is supported by our modeling results, as optimal predator
406 sizes are always a little larger than expected, based solely on the implemented preferred predator-

407 prey body size ratio (Figure 5). Since selection for mobility in the predator is largest in the most
408 resource-depleted and fragmented landscapes where herbivore abundances are lowest, the largest
409 predators are selected here. This pattern is general under a wide range of boundary conditions (see
410 sensitivity analysis) except for the scenario in which clutch size for the herbivore and predator is low.
411 When clutch size of the herbivore is low, the predator size is selected to be large when habitat is
412 abundant (P equaling 0.90 and $H = 1$) relative to when it is rare (P equaling 0.05 and $H = 1$). By
413 constraining clutch size, the growth speed of the herbivore population is lowered. As such, the
414 herbivore population growth rates are reduced, promoting predator mobility even when P is high.
415 This mechanism is confirmed by the observation that lowering resource growth speed within the
416 resource-herbivore model also resulted in selection of larger herbivores (Hillaert, Hovestadt, *et al.*,
417 2018). Under low P and low herbivore reproductive values, the largest predators can no longer
418 persist due to food limitation and selection turns towards smaller average predator sizes.

419 Our theoretical predictions are confirmed by some but not all experimental studies. For instance,
420 within a fine-grained fragmentation study, the density of the largest species of ground beetles
421 responded positively to fragmentation (Braschler and Baur, 2016). However, in other predatory
422 invertebrate species (spiders and rove beetles), response to fine-scale fragmentation was unrelated
423 to body size (Braschler and Baur, 2016). In another study, web spiders showed no response to
424 urbanization, which is associated with habitat fragmentation, whereas the community-weighted
425 average body size decreased with urbanization in ground beetles and ground spiders (Merckx *et al.*,
426 2018). These and other counterintuitive outcomes might be explained by confounding factors. For
427 instance, fragmentation due to urbanization is also linked with increasing temperatures by urban
428 warming (Merckx *et al.*, 2018). Further, body size responses to habitat fragmentation might strongly
429 be influenced by food web structure or the level of informed movement (Liao, Bearup and Blasius,
430 2017; Hillaert, Vandegehuchte, *et al.*, 2018). Generally, more experimental research on the effect of
431 fine-scale fragmentation on body size across trophic levels is necessary to validate theoretical

432 expectations, for instance by using the Metatron platform (i.e. an innovative infrastructure to study
433 terrestrial organism movement under semi-natural conditions , Legrand *et al.*, 2012).

434 Top-down versus bottom-up effects

435 Temporal and spatial dynamics of the resource and the herbivore are strongly influenced by the
436 predator. The predator clearly suppresses herbivore population sizes at local scales and this effect
437 cascades down the food web, resulting in a weaker control of the resource, which then locally
438 accumulates. At this point, the top-down force influences the bottom-up one by creating temporal
439 variation in resource abundance which imposes selection for larger and more mobile herbivores. This
440 insight provides an explanation of why in a recent meta-analysis, top-down forces were found to be
441 stronger than bottom-up forces for the fitness of terrestrial insect herbivores, considering that body
442 size largely influences the fitness of an individual (Vidal & Murphy, 2018; Peters, 1983). However, the
443 effect of bottom-up forces should not be underestimated. As highlighted by our modelling approach,
444 habitat loss and fragmentation results in a selection for larger predator individuals whereas
445 herbivore size does not respond. Consequently, predators are forced to consume herbivores that
446 deviate from their preferred optimal size. Furthermore, we should note that movement of herbivores
447 in our model is only influenced by the basal resource and not the predator, so non-lethal effects
448 acting in landscapes of fear are not considered (Bleicher, 2017; Schmitz *et al.*, 2017). Moreover, we
449 show that top-down and bottom-up act in concert and strongly interact. Without predators, habitat
450 fragmentation prevents the consumer from reaching an ideal free distribution, hence imposing
451 spatial variation in resource biomass (Hillaert, Vandegehuchte, *et al.*, 2018). As such, resources
452 biomass increases globally with habitat fragmentation and destruction when a predator is not
453 present. In contrast, when a predator is present, habitat fragmentation creates predator-free refuges
454 for the herbivore. This increases the percentage of cells being occupied by the herbivore, globally
455 controlling resource production. As such, habitat fragmentation and destruction decrease resource
456 amount in the presence of a predator.

457

458 Effect of habitat fragmentation on predator-herbivore body size ratio

459 Predators experience one extra selection pressure that is not experienced by the herbivore: predators
460 are selected to have a size that approximates the preferred ratio to maximize chance of successful
461 attack. Under the continuous availability of resources, in landscapes of $P = 0.9$ and $H = 1$, the selected
462 predator-herbivore body mass ratio approximates the preferred ratio. However, as only predator size
463 increases with habitat fragmentation, the available body mass distribution of herbivores deviates
464 from the preferred one when resources are spatially structured (Tsai, Hsieh and Nakazawa, 2016).
465 The realized predator-herbivore body mass ratio thus increases with habitat loss and fragmentation.
466 Hence, the realized predator-prey body mass ratios and coupled interaction strengths are altered
467 (Emmerson and Raffaelli, 2004). This model prediction coincides with the finding that prey limitation
468 determines variation in predator-prey body mass ratios between food webs (Costa-Pereira *et al.*,
469 2018). Further, selection pressures that enlarge differences between preferred and available body
470 mass distributions for predators might increase extinction rates of species from higher trophic levels.
471 Moreover, our sensitivity analysis indicates that when predators are intrinsically more mobile (e.g.
472 high t_m), their realized predator-prey body mass ratio deviate less from the preferred ratio in highly
473 fragmented landscapes. Whereas, when predators are intrinsically less mobile (e.g. low t_m), their
474 realized predator-prey body mass ratio deviate even more from the preferred ratio in these
475 landscapes.

476 The predicted deviation of the predator-prey body mass ratio from the implemented optimum does
477 consequently not only depend on the level of habitat fragmentation but also on the limitation by
478 resources and the species-specific mobility traits.

479

480 *Conclusion*

481 Our developed modeling framework, which merges principles from movement ecology and
482 metabolic theory, shows that the effects of habitat fragmentation and destruction on body size
483 distributions within food webs is not obvious. Predation selects for increased herbivore size by
484 generating spatial and temporal variation in the distribution of the resource, favoring herbivore
485 movement. As top-down forces dominate, the effect of predation should always be considered when
486 estimating the effect of habitat fragmentation on changing selection pressures in food webs (Liao,
487 Bearup and Blasius, 2017). Since predation results in larger optimal herbivore sizes in all landscape
488 types, herbivore size no longer increases with habitat fragmentation as observed in a simpler
489 consumer-resource food web. However, habitat fragmentation leads to larger optimal predator sizes
490 as herbivores become rarer, favoring gap-crossing abilities and hence, movement potential, of the
491 predator. Therefore, even if a herbivore and its predator persist under conditions of fine-scale
492 fragmentation, the realized predator-herbivore body mass ratios will be larger than in continuous
493 habitats. These deviations in realized predator-prey body mass ratios affect interaction strength,
494 which may cascade through the food web and alter the energy flow (Emmerson and Raffaelli, 2004).

495

496

497 *References*

- 498 Allen, C. R. *et al.* (2006) 'Patterns in body mass distributions: sifting among alternative hypotheses',
499 *Ecology Letters*, 9(5), pp. 630–643. doi: 10.1111/j.1461-0248.2006.00902.x.
- 500 Amarasekare, P. (2016) 'Evolution of dispersal in a multi-trophic community context', *Oikos*, 125(4),
501 pp. 514–525. doi: 10.1111/oik.02258.
- 502 Bartholomew, G. (1982) 'Energy metabolism', in Bartholomew, G. *et al.* (eds) *Animal Physiology:*
503 *Principles and Adaptations*. New York: Macmillan, pp. 57–110.
- 504 Bleicher, S. S. (2017) 'The landscape of fear conceptual framework: definition and review of current
505 applications and misuses', *PeerJ*, 5, p. e3772. doi: 10.7717/peerj.3772.
- 506 Braschler, B. and Baur, B. (2016) 'Diverse effects of a seven-year experimental grassland
507 fragmentation on major invertebrate groups', *PLoS ONE*, 11(2), pp. 1–20. doi:
508 10.1371/journal.pone.0149567.
- 509 Brose, U. *et al.* (2006) 'Consumer- Resource Body-Size Relationships In Natural Food Webs', *Ecology*,
510 87(10), pp. 2411–2417. doi: doi:10.1890/0012-9658(2006)87[2411:CBRINF]2.0.CO;2.
- 511 Brose, U. *et al.* (2008) 'Foraging theory predicts predator-prey energy fluxes', *Journal of Animal*
512 *Ecology*, 77(5), pp. 1072–1078. doi: 10.1111/j.1365-2656.2008.01408.x.
- 513 Brose, U. (2010) 'Body-mass constraints on foraging behaviour determine population and food-web
514 dynamics', *Funct Ecol*, 24(1), pp. 28–34. doi: 10.1111/j.1365-2435.2009.01618.x.
- 515 Brose, U. *et al.* (2017) 'Predicting the consequences of species loss using size-structured biodiversity
516 approaches', *Biological Reviews*, 92(2), pp. 684–697. doi: 10.1111/brv.12250.
- 517 Brose, U., Williams, R. J. and Martinez, N. D. (2006) 'Allometric scaling enhances stability in complex
518 food webs', *Ecology Letters*, 9(11), pp. 1228–1236. doi: 10.1111/j.1461-0248.2006.00978.x.
- 519 Brown, J. H. *et al.* (2004) 'Toward a metabolic theory of ecology', *Ecology*, 85(7), pp. 1771–1789. doi:

520 10.1890/03-9000.

521 Buchmann, C. M. *et al.* (2011) 'An allometric model of home range formation explains the structuring
522 of animal communities exploiting heterogeneous resources', *Oikos*, 120(1), pp. 106–118. doi:
523 10.1111/j.1600-0706.2010.18556.x.

524 Buchmann, C. M. *et al.* (2013) 'Habitat loss and fragmentation affecting mammal and bird
525 communities—The role of interspecific competition and individual space use', *Ecological Informatics*.
526 Elsevier B.V., 14, pp. 90–98. doi: 10.1016/j.ecoinf.2012.11.015.

527 Buddenbrock, W. V. (1934) 'Über die kinetische und statische Leistung grosser und kleiner Tiere und
528 ihre bedeutung für dem Gesamtstoffwechsel', *Naturwissenschaft*, 22, pp. 675–680.

529 Cattarino, L., McAlpine, C. A. and Rhodes, J. R. (2016) 'Spatial scale and movement behaviour traits
530 control the impacts of habitat fragmentation on individual fitness', *Journal of Animal Ecology*, 85(1),
531 pp. 168–177. doi: 10.1111/1365-2656.12427.

532 Costa-Pereira, R. *et al.* (2018) 'Prey Limitation Drives Variation in Allometric Scaling of Predator-Prey
533 Interactions', *The American Naturalist*, 192(4), pp. E139–E149. doi: 10.1086/698726.

534 Delgado, M. M. *et al.* (2014) 'Prospecting and dispersal: their eco-evolutionary dynamics and
535 implications for population patterns', *Proceedings of the Royal Society B: Biological Sciences*,
536 281(1778), pp. 20132851–20132851. doi: 10.1098/rspb.2013.2851.

537 Delong, J. P. and Vasseur, D. A. (2012) 'Size-density scaling in protists and the links between
538 consumer-resource interaction parameters', *Journal of Animal Ecology*, 81(6), pp. 1193–1201. doi:
539 10.1111/j.1365-2656.2012.02013.x.

540 Elton, C. (1927) *Animal Ecology*. 2001st edn. The University of Chicago Press.

541 Emmerson, M. C. and Raffaelli, D. (2004) 'Predator – prey body size , interaction strength and the
542 stability of a real food web', pp. 399–409.

- 543 Etherington, T. R., Holland, E. P. and O'Sullivan, D. (2015) 'NLMpy: A python software package for the
544 creation of neutral landscape models within a general numerical framework', *Methods in Ecology
545 and Evolution*, 6(2), pp. 164–168. doi: 10.1111/2041-210X.12308.
- 546 Etienne, R. S. and Olf, H. (2004) 'How Dispersal Limitation Shapes Species-Body Size Distributions in
547 Local Communities', *The American Naturalist*, 163(1), pp. 69–83. doi: 10.1086/380582.
- 548 Fahrig, L. (2017) 'Ecological Responses to Habitat Fragmentation Per Se', *Annual Review of Ecology,
549 Evolution, and Systematics*, 48(1), p. annurev-ecolsys-110316-022612. doi: 10.1146/annurev-ecolsys-
550 110316-022612.
- 551 Fletcher Jr, R. J. *et al.* (2018) 'Is habitat fragmentation good for biodiversity?', *Biological
552 Conservation*. Elsevier, 226(April), pp. 9–15. doi: 10.1016/j.biocon.2018.07.022.
- 553 Fritschie, K. J. and Olden, J. D. (2016) 'Disentangling the influences of mean body size and size
554 structure on ecosystem functioning: An example of nutrient recycling by a non-native crayfish',
555 *Ecology and Evolution*, 6(1), pp. 159–169. doi: 10.1002/ece3.1852.
- 556 Grimm, V. *et al.* (2010) 'The ODD protocol: A review and first update', *Ecological Modelling*. Elsevier
557 B.V., 221(23), pp. 2760–2768. doi: 10.1016/j.ecolmodel.2010.08.019.
- 558 Hastings, A. (1983) 'Can spatial variation alone lead to selection for dispersal?', *Theoretical
559 Population Biology*, 24(3), pp. 244–251. doi: 10.1016/0040-5809(83)90027-8.
- 560 Hillaert, J., Vandegheuchte, M. L., *et al.* (2018) 'Information use during movement regulates how
561 fragmentation and loss of habitat affect body size', *Proceedings of the Royal Society B: Biological
562 Sciences*, 285(1884), p. 20180953. doi: 10.1098/rspb.2018.0953.
- 563 Hillaert, J., Hovestadt, T., *et al.* (2018) 'Size-dependent movement explains why bigger is better in
564 fragmented landscapes', *Ecology and Evolution*. doi: 10.1002/ece3.4524.
- 565 Hirt, M. R. *et al.* (2017) 'The little things that run: a general scaling of invertebrate exploratory speed

- 566 with body mass', *Ecology*, 98(11), pp. 2751–2757. doi: 10.1002/ecy.2006.
- 567 Holling, C. S. (1992) 'Cross-Scale Morphology, Geometry, and Dynamics of Ecosystems', *Ecological*
568 *Monographs*, 62(4), pp. 447–502. doi: 10.2307/2937313.
- 569 Howeth, J. G. *et al.* (2013) 'Intraspecific phenotypic variation in a fish predator affects multitrophic
570 lake metacommunity structure', *Ecology and Evolution*, 3(15), pp. 5031–5044. doi:
571 10.1002/ece3.878.
- 572 Jackson, H. B. and Fahrig, L. (2013) 'Habitat Loss and Fragmentation', *Encyclopedia of Biodiversity:*
573 *Second Edition*, 4, pp. 50–58. doi: 10.1016/B978-0-12-384719-5.00399-3.
- 574 Jackson, H. B. and Fahrig, L. (2015) 'Are ecologists conducting research at the optimal scale?', *Global*
575 *Ecology and Biogeography*, 24(1), pp. 52–63. doi: 10.1111/geb.12233.
- 576 Legrand, D. *et al.* (2012) 'The Metatron: an experimental system to study dispersal and
577 metaecosystems for terrestrial organisms', *Nature Methods*, 9(8), pp. 828–833. doi:
578 10.1038/nmeth.2104.
- 579 Liao, J., Bearup, D. and Blasius, B. (2017) 'Food web persistence in fragmented landscapes',
580 *Proceedings of the Royal Society B: Biological Sciences*, 284(1859), p. 20170350. doi:
581 10.1098/rspb.2017.0350.
- 582 Lomolino, M. V. and Perault, D. R. (2007) 'Body size variation of mammals in a fragmented,
583 temperate rainforest', *Conservation Biology*, 21(4), pp. 1059–1069. doi: 10.1111/j.1523-
584 1739.2007.00727.x.
- 585 McCann, K. S. (2012) *Food webs*. Edited by S. A. Levin and H. S. Horn. Princeton Univ. Press.
- 586 Merckx, T. *et al.* (2018) 'Body-size shifts in aquatic and terrestrial urban communities', *Nature*.
587 Springer US, (iDiv), p. 1. doi: 10.1038/s41586-018-0140-0.
- 588 Milne, B. T. *et al.* (1992) 'Interactions between the fractal geometry of landscapes and allometric

- 589 herbivory', *Theoretical Population Biology*, 41(3), pp. 337–353. doi: 10.1016/0040-5809(92)90033-P.
- 590 Moses, M. E. *et al.* (2008) 'Revisiting a model of ontogenetic growth: estimating model parameters
591 from theory and data.', *The American naturalist*, 171(5), pp. 632–645. doi: 10.1086/587073.
- 592 Nash, K. L. *et al.* (2014) 'Habitat structure and body size distributions: Cross-ecosystem comparison
593 for taxa with determinate and indeterminate growth', *Oikos*, 123(8), pp. 971–983. doi:
594 10.1111/oik.01314.
- 595 Neel, M. C., McGarigal, K. and Cushman, S. A. (2004) 'Behavior of class-level landscape metrics across
596 gradients of class aggregation and area', *Landscape Ecology*, 19(4), pp. 435–455. doi:
597 10.1023/B:LAND.0000030521.19856.cb.
- 598 Otto, S. B., Rall, B. C. and Brose, U. (2007) 'Allometric degree distributions facilitate food-web
599 stability', *Nature*, 450(7173), pp. 1226–1229. doi: 10.1038/nature06359.
- 600 Pawar, S., Dell, A. I. and Van M. Savage (2012) 'Dimensionality of consumer search space drives
601 trophic interaction strengths', *Nature*. Nature Publishing Group, 486(7404), pp. 485–489. doi:
602 10.1038/nature11131.
- 603 Peters, R. H. (1983) *The ecological implications of body size*, *Cambridge studies in ecology*. Edited by
604 E. Beck, H. J. B. Birks, and E. F. Connor. Cambridge: Cambridge University Press. doi:
605 10.1017/CBO9780511608551.
- 606 Poethke, H. J. and Hovestadt, T. (2002) 'Evolution of density- and patch-size-dependent dispersal
607 rates.', *Proceedings. Biological sciences / The Royal Society*, 269(1491), pp. 637–45. doi:
608 10.1098/rspb.2001.1936.
- 609 Portalier, S. M. J. *et al.* (2018) 'The mechanics of predator-prey interactions: first principles of physics
610 predict predator-prey size ratios', *bioRxiv*. Available at:
611 <http://biorxiv.org/content/early/2018/05/03/313239.abstract>.

- 612 Raffaelli, D. *et al.* (2016) 'The textural discontinuity hypothesis: An exploration at a regional level.
613 Shortened version: Exploring Holling's TDH', *Oikos*, 125(6), pp. 797–803. doi: 10.1111/oik.02699.
- 614 Renauld, M. *et al.* (2016) 'Landscape Simplification Constrains Adult Size in a Native Ground-Nesting
615 Bee', *PLOS ONE*. Edited by G. Smagghe, 11(3), pp. 1–11. doi: 10.1371/journal.pone.0150946.
- 616 Ricklefs, R. E. (1974) 'Energetics of reproduction in birds', in Paynter, R. A. (ed.) *Avian energetics*.
617 Cambridge, Massachusetts: Nuttall Ornithological Club, pp. 152–297.
- 618 Schmitz, O. J. *et al.* (2017) 'Toward a community ecology of landscapes: predicting multiple predator–
619 prey interactions across geographic space', *Ecology*, 98(9), pp. 2281–2292. doi: 10.1002/ecy.1916.
- 620 Tsai, C. H., Hsieh, C. H. and Nakazawa, T. (2016) 'Predator–prey mass ratio revisited: does preference
621 of relative prey body size depend on individual predator size?', *Functional Ecology*, 30(12), pp. 1979–
622 1987. doi: 10.1111/1365-2435.12680.
- 623 Warzecha, D. *et al.* (2016) 'Intraspecific body size increases with habitat fragmentation in wild bee
624 pollinators', *Landscape Ecology*, 31, pp. 1449–1455. doi: 10.1007/s10980-016-0349-y.
- 625 West, G. B., Brown, J. H. and Enquist, B. J. (2001) 'A general model for ontogenetic growth', *Nature*,
626 413(6856), pp. 628–631. doi: 10.1038/35098076.
- 627 Yeakel, J. D., Kempes, C. P. and Redner, S. (2018) 'Dynamics of starvation and recovery predict
628 extinction risk and both Damuth's law and Cope's rule', *Nature Communications*, 9(1), pp. 1–10. doi:
629 10.1038/s41467-018-02822-y.

630

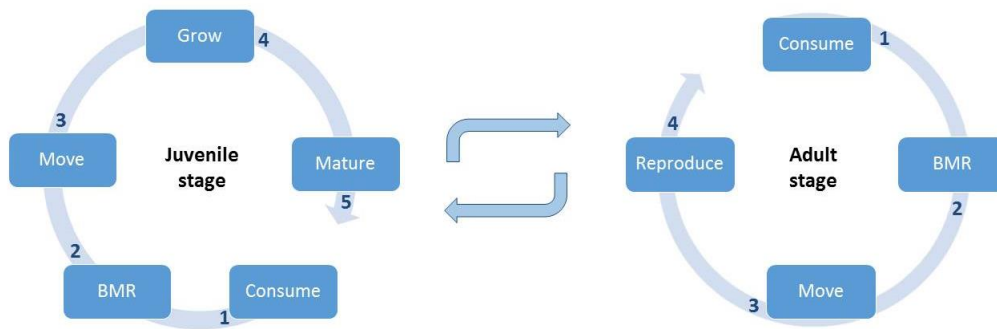
631 *Acknowledgements*

632 JH was supported by Research Foundation – Flanders (FWO). The computational resources (STEVIN
633 Supercomputer Infrastructure) and services used in this work were kindly provided by Ghent

634 University, the Flemish Supercomputer Center (VSC), the Hercules Foundation and the Flemish
635 Government – department EWI.

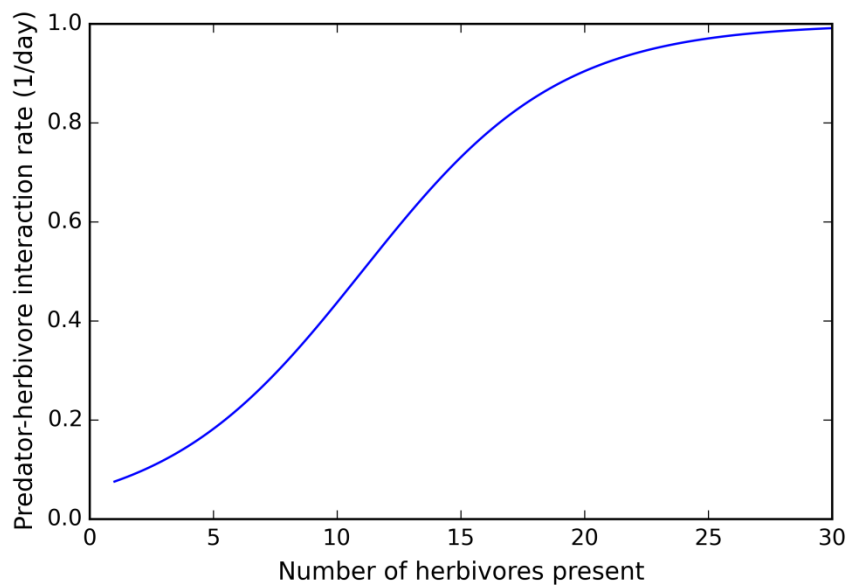
636

637 *Figures*



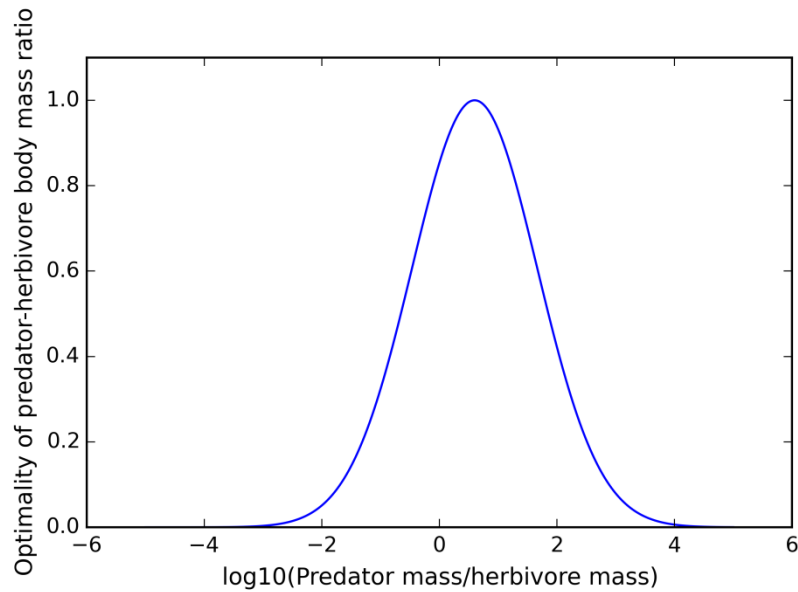
638

639 *Figure 1: A comparison of daily events for the juvenile and adult stage of the herbivore and the predator (Hillaert,*
640 *Vandegehuchte, et al., 2018). BMR stands for basal metabolic rate costs. Numbers highlight the ordering of events within a*
641 *day.*



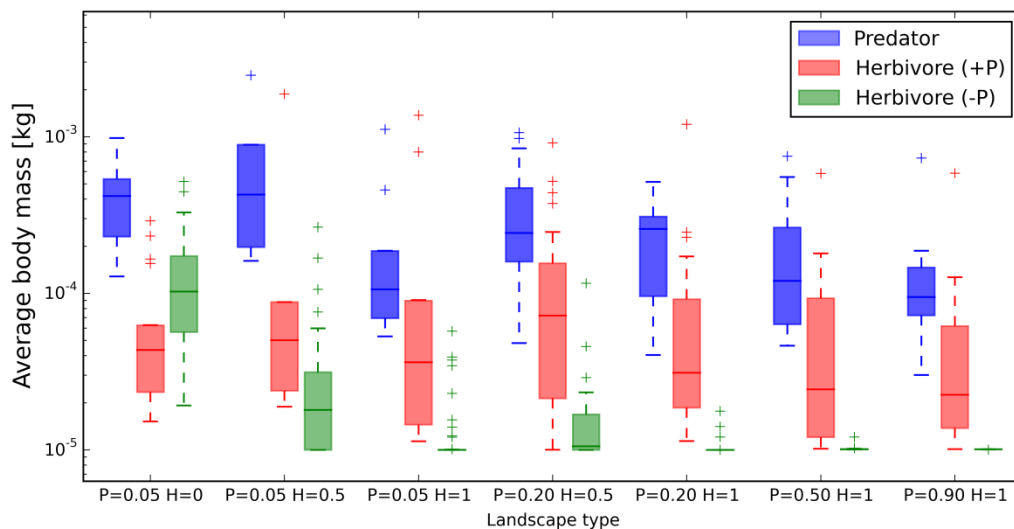
642

643 *Figure 2: Relationship between predator-herbivore interaction rate and number of herbivores present within a cell. During a*
644 *day, the number of herbivores present in a cell is constantly updated.*



645

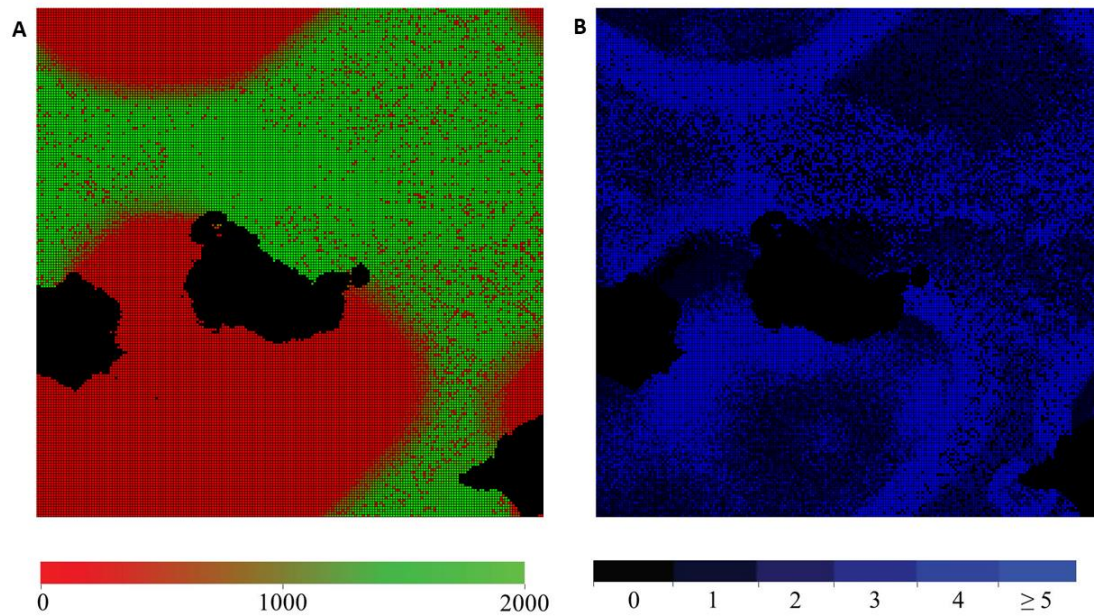
646 *Figure 3: The implemented optimal predator-herbivore body size ratio is displayed. This distribution is observed by Brose*
647 *(2006) to occur in terrestrial systems for invertebrate predators.*



648

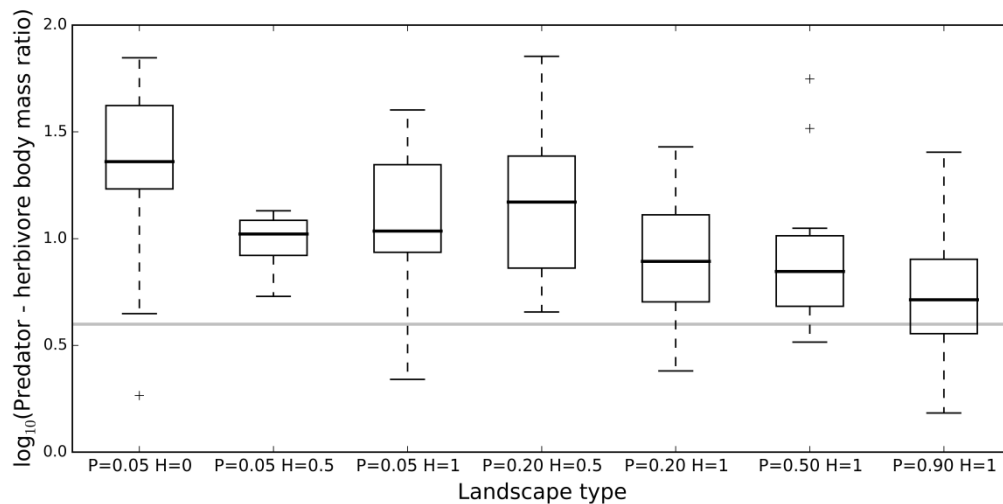
649 *Figure 4: The effect of habitat loss and fragmentation of a resource on average body mass of its herbivore and a predator. In*
650 *order to infer the effect of predation, average herbivore body mass is also displayed for a scenario in which the predator was*
651 *not present (see legend). For an overview of the number of simulations per scenario, see Table S2.1 in supplementary*
652 *material part 2. An overview of the parameter settings is given in Table S1.1 in supplementary material part 1.*

653



654

655 *Figure 5: Spatial distribution of the herbivore (number of individuals) and resource (in Joule) within one simulation with P*
 656 *equaling 0.90 and H 1 when a predator is present. A) The distribution of resources is displayed (black: unsuitable habitat)*
 657 *and B) the distribution of herbivores (black: no herbivores present).*



658

659 *Figure 6: The effect of habitat loss and fragmentation on average realized predator-herbivore body mass ratios. The*
 660 *horizontal line represents the preferred predator-herbivore body mass ratio maximizing the predators' foraging success. For*
 661 *an overview of the number of simulations per scenario, see Table S2.1 in supplementary material part 2. An overview of the*
 662 *parameter settings is given in Table S1.1 in supplementary material part 1.*

